Title
Evaluation of bi-layer silk fibroin grafts for onlay urethroplasty in a rabbit model of urethral stricture disease

Journal
Regenerative Medicine, ahead-of-print(ahead-of-print)

ISSN
1746-0751

Authors
Gundogdu, Gokhan
Budrewicz, Jay
Giordano, Jodie
et al.

Publication Date
2024-08-30

DOI
10.1080/17460751.2024.2389753

Peer reviewed

Regenerative Medici

Evaluation of Bi-layer Silk Fibroin Grafts for Onlay Urethroplasty in a Rabbit Model of Urethral Stricture Disease

Journal:	*Regenerative Medicine*
Manuscript ID	RME-2024-0038.R2
Manuscript Type:	Research Article
Keywords:	urethra, Tissue engineering, silk fibroin, biomaterial, urethroplasty

Abstract

Background: Autologous tissues such as buccal mucosa (BM) are widely used for reconstruction of urethral strictures, however limitations such as donor site morbidity and scarce tissue supply require the development of alternative biomaterials for urethral repair. The goals of this study were to determine the safety and efficacy of bi-layer silk fibroin (BLSF) matrices for urethral stricture repair and compare histological and functional outcomes to the standard approach, BM urethroplasty under good laboratory practices. **Material and Methods:** 13 rabbits exhibiting urethral stricture formation following electrocoagulation injury were treated with onlay urethroplasty with either acellular BLSF (N=7) or autologous BM (N=6) grafts for 3 months. Uninjured control rabbits were maintained in parallel (N=4). **Results and Conclusions:** Animals receiving BLSF implants were demonstrated to be functionally equivalent to BM grafts in their ability to restored strictured calibers, support micturition and promote tissue regeneration with minimal inflammation.

Plain Language Summary: Non applicable.

Tweetable Abstract: Non applicable.

Graphical Abstract: Non applicable.

Video Abstract: Non applicable.

Keywords: urethra, tissue engineering, silk fibroin, biomaterial, urethroplasty

Introduction

Urethral stricture disease (USD) is a debilitating pathology that occurs due to ischemic spongiofibrosis resulting in narrowing of the urethral lumen and subsequent obstruction of the urinary tract [1]. Urethral strictures arise from a multitude of etiologies including iatrogenic secondary to prolonged catheterization or transurethral instrumentation damage, chronic infection with sexually transmitted diseases, inflammatory conditions such as lichen sclerosis, aberrant wound healing following straddle injuries or pelvic fractures, and idiopathic or developmental abnormalities [2]. This condition is highly prevalent in males (~400 per 100,000) with increased frequency in patients after 55 years of age [3]. USD complications include recurrent urinary tract infections, urinary retention, hydronephrosis, and ultimately renal failure if left untreated [4,5].

Primary management of short urethral strictures (<2 cm in length) is traditionally accomplished with endoscopic methods including cold knife or holmium laser internal urethrotomy and dilation [6,7]. Due to high rates of stricture recurrence, these approaches are not recommended for repair of longer strictures (>2 cm in length) or short strictures which have failed primary endoscopic management [8,9]. In these cases, onlay or tubularized urethroplasty with autologous tissue grafts such as buccal mucosa represent the gold standard [10]. However, buccal mucosal urethroplasty is associated with complication rates up to 37% and recurrence rates which can exceed 20% for strictures 4-8 cm in length [11]. In addition, the use of buccal mucosal grafts for urethral repair also necessitates secondary surgical procedures for tissue procurement which can lead to significant donor site morbidity hampering quality of life [12]. These studies emphasize the need for superior graft configurations which can overcome the need for secondary procurement procedures and the negative consequences of buccal mucosa for urethral reconstruction.

A variety of acellular and cell-seeded biomaterials composed of decellularized tissues or synthetic polyester meshes have been investigated in animal models and clinical studies as substitutes for the use of buccal mucosa in urethroplasty [13-16]. However, these implant designs have not been widely adopted into clinical

practice due to suboptimal in vivo outcomes including fibrosis, stricture recurrence and graft contracture [17-22]. Currently, there is no FDA-approved surgical graft for urethral reconstruction. Previous findings from our research team suggest that bi-layer silk fibroin (BLSF) biomaterials may serve as alternative biodegradable platforms for urethroplasty due to their high structural strength and elasticity, controllable degradation and low immunogenicity [23]. In rabbit models of urethral repair, these multi-functional, acellular implants have been reported to promote defect consolidation and maintenance of organ continuity via a fluid-tight film layer, while supporting host tissue integration and intrinsic regenerative processes within a porous foam compartment [24,25]. The goal of the present study was to compare the performance of BLSF matrices with autologous buccal mucosa grafts for onlay urethroplasty in a rabbit model of USD under good laboratory practices (GLP) as a step toward clinical translation.

Materials and Methods

Biomaterials

BLSF scaffolds (**Figure 1E, inset**) were fabricated from aqueous *Bombyx mori* silk fibroin solutions (Canon Virginia, Inc, Newport News, VA) at the Southwest Research Institute (San Antonio, TX) employing a solvent-casting/salt-leaching procedure in tandem with silk fibroin (SF) film casting as previously described using ISO-13485 standards [26]. The structural and mechanical properties of BLSF grafts have been reported in published studies [26]. Biomaterials were autoclave sterilized prior to surgical procedures.

Study Site and GLP

The animal study and all outcome analyses were conducted at CBSET (Lexington, MA) under the guidance of an independent facility study director in compliance with the Food and Drug Administration Good Laboratory Practice (GLP) Regulations, as set forth in Title 21 of the United States Code of Federal Regulations, Part 58 with the exception that Microsoft Excel and SigmaPlot® software were used for data calculations and statistical analyses, respectively. The test facility's quality assessment unit was independent of the personnel engaged in the direction and conduct of the study, and adequately inspected critical phases of the study at the test facility to assure the integrity of the study as required by the regulations stated above.

Animals

Twenty male, New Zealand white rabbits (6 months of age, 2.36-3.26 kg, Envigo, Denver, PA) were employed in this study and housed according to the standards set forth in the National Institutes of Health's Guidelines for the Care and Use of Laboratory Animals [27]. Animals were supplied Purina Lab Diet (#5326 Laboratory Rabbit Diet HF), hay and potable water ad libitum. All animal procedures and husbandry practices were reviewed and approved by the CBSET, Inc. Institutional Animal Care and Use Committee (IACUC) under Protocol I00349 and were in compliance with the Animal Welfare Act and the United States Department of Agriculture regulations [28-30]. Sixteen rabbits were subjected to stricture creation via urethral electrocoagulation and those demonstrating >30% urethral stenosis (N=13) were then treated with onlay urethroplasty with either acellular BLSF scaffolds (N=7) or autologous buccal mucosal grafts (N=6) for a 3 month implantation period. Uninjured rabbits (N=4) were maintained in parallel as longitudinal controls.

Surgical Procedures

Anesthesia and Perioperative Procedures

Prior to surgery, animals received a combined subcutaneous injection of Ketamine (25 mg/kg) and Xylazine (5 mg/kg) for induction of anesthesia. Isoflurane anesthesia was then administered and maintained via endotracheal inhalation and supportive fluids were delivered via an intravenous catheter. An ophthalmic lubricant was also applied to the eyes. For electrocoagulation injury and urethroplasty procedures, pre-emptive analgesia with subcutaneous buprenorphine (0.01 mg/kg) was performed. Animals also received subcutaneous Baytril (5.0 mg/kg) and oral Meloxicam (0.3 mg/kg) to mitigate bacterial infections and inflammation, respectively.

Urethral Electrocoagulation Injury

Rabbits were oriented in a supine position, excess fur surrounding the genitalia was trimmed, and the surgical field was aseptically prepared and draped. A 5-0 polyprolene stay suture was positioned at the tip of the distal penile skin to facilitate surgical maneuvers. Following a baseline retrograde urethrogram, initial uninjured urethra luminal images were acquired by a pediatric cystoscope. A 4 French ureteral catheter was then introduced into the urethra and followed by a 7.9 French pediatric resectoscope. An electrocoagulation injury (1/2 of the transverse perimeter and 2 cm in length) in the anterior urethral spongiosum was performed from the 3-9 o'clock position ~2 cm proximal to the external meatus by using an electrosurgical hook from a pediatric resectoscope under direct urethroscopic visualization (**Figure 1A**). After urethral injury, an 8 French Zaontz urethral stent was introduced into the urethra and was fixed to the glans with 5-0 polypropylene sutures. Rabbits were fitted with Elizabethan collars to prevent self-mutilation and free urine drainage via catheterization was maintained for 1 week post-operatively. Animals were allowed to voluntary void after the catheterization period. Urethroplasty procedures were carried out 13-16 days following electrocoagulation injury as described below.

Onlay Urethroplasty

A retrograde urethrogram followed by urethroscopic examination was performed to characterize the severity and length of urethral strictures in all animals prior to reconstruction. For buccal mucosa urethroplasty, autologous tissues were extracted from the jugal region of the rabbit's oral cavity (**Figure 1B**). The donor site was exposed with interrupted stitches using 5-0 stay sutures. A vasoconstrictor (1% Lidocaine HCl with epinephrine [1:200,000]) was injected locally into the submucosa facilitating the resection of a 1 cm^2 buccal mucosa fragment. The wound was not sutured and left to spontaneously heal. Onlay urethroplasty procedures were then performed as previously reported [25]. Briefly, a stay suture was placed at the glans penis. The scrotal web was incised, and the ventral penile skin was opened longitudinally. A short segment of the proximal penile urethra was dissected from the penile corporal body and a vessel loop was placed on the proximal urethra for bleeding control. An 8 French Zaontz urethral stent was introduced into the urethra. The stenotic urethral segment was incised, and fibrotic ventral urethral wall was resected to create a ~2 cm x ~0.5 cm (length x width) elliptical defect (**Figure 1C**). Buccal mucosal or BLSF grafts of comparable size to the injury site were sutured within the defect with 6-0 absorbable sutures (**Figure 1D, E**). Nonabsorbable 6-0 marking sutures were placed laterally and along the proximal/distal edges of the graft for identification of the original implant region. The 8 French Zaontz stent was fixed to the glans tip and catheterization was maintained for 7 days post-operatively after which voluntary voiding was permitted. The skin was closed by 5-0 resorbable interrupted sutures and Bupivacaine infiltration (up to 1 mg/kg; subcutaneously) was administered for pain control. Rabbits were maintained for 3 months and evaluated for study endpoints described below.

Retrograde urethrography (RUG) and urethroscopy

Longitudinal urethroscopic and RUG analyses were carried out as previously described [25]. Rabbits were evaluated prior to surgical injury to establish baseline urethral anatomy, 13-16 days following electrocoagulation to characterize the degree of stricture formation, and at 3 months post-repair to assess organ continuity. Under general anesthesia, the genitalia were aseptically prepared and the surgical area was draped in sterile fashion. A 5-0 polypropylene stay suture was placed at the tip of glans. A 14-gauge IV catheter was inserted ~1 cm into the urethra and fixed by a torniquet. A sterile fluid line was connected and contrast medium was instilled into the urethral meatus from a ~100 cm height. Fluoroscopic images were taken in anterior-posterior (AP) and oblique directions to visualize urethra. Luminal urethral images encompassing the surgical site were acquired with a pediatric cystoscope and video processor. Relative urethral calibers in experimental groups across all timepoints described above were determined from RUG images using Centricity® Cardiology CA1000 Cardiac Review 2.0 software following size calibration with a 14-gauge angiocatheter. Relative urethral calibers were determined by calculating the percentage of luminal urethral diameter at injured/repaired positions relative to an uninjured distal segment.

Histological and histomorphometric analyses

Following euthanasia and necropsy, penile segments isolated from uninjured controls and rabbits receiving implants were subjected to routine histological processing. Specimens were fixed in 10% neutral-buffered formalin, dehydrated in graded alcohols, and paraffin embedded. Sections (5 μm) from central and peripheral regions of implant and control replicates were cut and stained with hematoxylin and eosin (H&E) as well as Masson's trichrome (MTS) using standard methods. Histomorphometric analyses were performed on stained specimens (1 field per region for each animal) by a blinded pathologist to score various parameters that reflect the extent of host responses including overall inflammation, inflammatory cell type, submucosal hemorrhage, fibrosis, necrosis and degree of epithelialization using previously published methods [31].

Statistical Evaluations

Statistical evaluations of quantitative data between groups were performed with the Mann-Whitney Rank Sum Test using SigmaPlot® statistical software with a value of $p<0.05$ defined as significant. Quantitative data were reported as means ± standard deviations (SD).

Results

All rabbits survived until scheduled euthanasia and demonstrated no evidence of severe intraoperative or postoperative complications following primary electrocoagulation injury or subsequent urethral reconstructive manipulations. Rabbits in each implant group were also capable of voluntary voiding following 1 week periods of catheterization after each surgical procedure. Prior to urethroplasty, urethroscopic and RUG analyses (**Figure 2**) revealed urethral stricture formation with >30% stenosis in 81% (N=13/16) of rabbits with a significant mean 44±13% reduction in relative urethral caliber compared to pre-operative baseline measurements (baseline vs stricture, $p<0.00001$). In addition, the mean length of urethral strictures was 2.2±0.5 cm. Longitudinal RUG assessments (**Figure 2**) of urethral segments reconstructed with buccal mucosal and BLSF grafts at 3 months post-op demonstrated a mean 102±22% and 100±19% recovery of the original urethral caliber, respectively (baseline vs post-repair buccal mucosa, $p=0.07$; baseline vs post-repair BLSF, $p=0.70$). In addition, normal urethral anatomy similar to uninjured controls was also observed in both graft groups with no evidence of contrast extravasation or fistula formation. Moreover, there was no significant difference in the relative urethral calibers between the repaired cohorts at this timepoint (post-repair buccal mucosa vs post-repair BLSF, $p=0.83$). These

results demonstrate that buccal mucosal and BLSF grafts are functionally equivalent for onlay urethroplasty and can restore urethral continuity of strictured segments.

At 3 months post-op, necropsy evaluations revealed host tissue ingrowth covering the implant site in both repaired groups with negligible contraction observed between the proximal/distal or lateral marking sutures. Histological (**Figure 3**) and histomorphometric (**Figure 4**) analyses were then carried out to characterize host tissue responses and extent of tissue regeneration in reconstructed urethral segments. De novo urethral tissue was observed spanning the original implant area in both graft cohorts with no evidence of residual BLSF matrix fragments or native buccal mucosa. Cross-sectional tissue architecture in repaired regions from each implant group resembled uninjured controls and contained a pseudostratified columnar epithelium covering an extracellular matrix (ECM)-rich, vascularized lamina propria surrounded by smooth muscle bundles. Overall inflammation scores were minimal (Scores <1.0) and statistically comparable between implant groups (post-repair buccal mucosa vs post-repair BLSF, p=0.53) with marginal elevation in reconstructed tissues compared to controls. Inflammatory cell types such as heterophils, histiocytes, lymphocytes, and plasma cells were present in the majority of study replicates with no significant difference between reconstructed cohorts (post-repair buccal mucosa vs post-repair BLSF, p>0.05), while fibrosis and necrosis were not detected in neotissues or controls. Low levels (Scores <1.0) of superficial epithelial erosion coupled with submucosal hemorrhage were also observed in both implant groups to comparable extents (post-repair buccal mucosa vs post-repair BLSF, p>0.05) and were presumably due to post-mortem tissue manipulation. Taken together, our data reveal that BLSF scaffolds support urethral tissue regeneration and elicit host tissue responses similar to autologous buccal mucosal grafts following urethral reconstruction.

Discussion

Previous non-GLP evaluations of BLSF scaffolds have demonstrated their potential for onlay urethroplasty in various preclinical settings [24,25]. In particular, these matrices were found to promote the formation of innervated, vascularized urethral tissues over the course of 3 months of implantation with restoration of urethral continuity and functional voiding in animal models of both acute trauma [24] and USD [25]. In addition, parallel in vivo assessments with conventional decellularized tissue scaffolds such as small intestinal submucosa (SIS) have also shown that BLSF biomaterials exhibit superior biocompatibility with significantly less chronic inflammatory reactions in regenerated urethral tissues [24]. Therefore, the aims of the current report were to determine the safety and efficacy of BLSF grafts for reconstruction of urethral strictures in rabbits and compare histological and functional outcomes to the standard surgical approach, buccal mucosal urethroplasty under GLP. An established male rabbit model of USD was employed in our studies given the similarities of urethral anatomy with humans as well as the propensity of this species to acquire USD following electrocoagulation injury [25,32-35].

Overall, BLSF implants were found to be safe for onlay urethroplasty with a 100% survival rate and no complications noted in reconstructed animals. These matrices were also demonstrated to be functionally equivalent to autologous buccal mucosal grafts in their propensity to restore strictured calibers, support micturition and promote de novo urethral tissues with minimal inflammatory reactions and foreign body responses. Moreover, no significant differences were noted between the implant groups for any study outcome, thus providing evidence that BLSF and buccal mucosal cohorts are similar in their ability to regenerate short urethral defects. However, BLSF grafts circumvent the need for autologous tissue harvest and therefore serve as an off-the-shelf option for urethral reconstruction while avoiding the risk of donor site morbidity. The use of acellular BLSF grafts for urogenital reconstruction also provides benefits over cell-seeded scaffolds by

eliminating the need for secondary surgeries for cell procurement as well as laboratory infrastructure required for cell expansion and construct development [36].

BLSF grafts exhibit a number of potential advantages over conventional decellularized tissue matrices and synthetic polyester meshes for urethral tissue engineering. For instance, the structural, mechanical and degradative properties of BLSF biomaterials can be further modified via adjustments in processing parameters such as silk fibroin content and porogen size to maximize host tissue ingrowth and functional performance [37-39]. In contrast, the physical properties of biomaterials derived from decellularized tissues are dependent upon the attributes of the source tissue as well as decellularization protocols [40] and therefore they have limited capacity to modulate bulk scaffold characteristics to optimize regenerative outcomes. In respect to polyester-based matrices, SF biomaterials such as BLSF grafts are less immunogenic and degrade into naturally occurring amino acids [41,42]. This is in contrast to polyester scaffold configurations which produce acidic degradation byproducts known to elicit chronic inflammatory responses in vivo which can compromise organ function due to adverse foreign body reactions [43]. The processing flexibility and low immunogenicity of BLSF grafts make them ideal candidates for the design of urethral implants with high translational potential.

Conclusions

Urethroplasty with BLSF grafts may serve as a new surgical strategy for patients with contraindications for buccal mucosal surgery including those with a history of leukoplakia, oral cancer or systemic dermatoses involving the oral cavity [44]. Future studies will focus on evaluating the efficacy of BLSF biomaterials for repair of long urethral strictures >2 cm in length given the average stricture length in men has been reported to be 4.8 cm [45]. In particular, in vivo assessments of BLSF grafts for urethroplasty in recently developed male and female porcine models of long urethral strictures [46] will be performed to determine the potential of these biomaterials to facilitate reconstruction of clinically relevant, urethral defects. Furthermore, investigations into the performance of BLSF grafts for tubular urethroplasty are also warranted to assess their potential utility in patients with a fibrotic urethral plate such as those afflicted with lichen sclerosis or previous failed hypospadias repair [47,48]. In summary, BLSF biomaterials represent emerging alternatives to buccal mucosal grafts for urethral repair.

Article Highlights

- Donor site morbidity and scarce tissue supply limit the efficacy of buccal mucosal grafts for urethral stricture repair.
- Bi-layer silk fibroin grafts represent potential alternatives for urethral reconstruction due to their mechanical robustness and low immunogenicity.
- Bi-layer silk fibroin implants were found to be functionally equivalent to buccal mucosal grafts in their capacity to restore continuity of strictured segments, promote tissue regeneration and support micturition in a rabbit model of urethral stricture disease and repair.

Figure Legends

Figure 1. Rabbit model of urethral stricture disease and urethroplasty. [**A**] Urethroscopic view of urethral mucosa during electrocoagulation injury. [**B**] Autologous buccal mucosa harvest with inset showing implant

dimensions. [**C**] Creation of urethral defect. [**D, E**] Ventral onlay urethroplasty with buccal mucosal graft [D] and bilayer silk fibroin (BLSF) scaffold [E] following stricture formation. Inset in [E]: BLSF matrix prior to implantation.

Figure 2. Imaging evaluations of urethral injury and repair responses. [**A, B**] Longitudinal retrograde urethrographic (RUG) analysis [Anterior/Posterior (AP) and oblique views] of representative animals at pre-operative baseline, after electrocoagulation injury demonstrating stricture formation (brackets), and at 3 months post-repair with buccal mucosal (BMG) [A] or bi-layer silk fibroin (BLSF) [B] grafts. Insets: urethroscopic images of repaired urethras at harvest. [**C**] Quantitation of relative urethral calibers calculated from RUG evaluations. Means ± standard deviation. (*) = $p<0.05$ compared to respective pre-operative baseline. (#) = $p>0.05$ compared to respective pre-operative baseline. (θ), $p=0.83$ in comparison to rabbits reconstructed with BMG grafts. Data in Panel C was acquired from N=4–7 animals per experimental group.

Figure 3. Histological evaluations of urethral neotissues and controls. [**A, B**] Photomicrographs of representative urethral cross-sections from rabbits repaired with buccal mucosal (BMG) or bi-layer silk fibroin (BLSF) grafts at 3 months post-op as well as controls stained with Masson's trichrome [A] and hematoxylin and eosin [B]. Axial periphery and central views of neotissues and controls are displayed in all panels. Brackets and asterisks denote reconstructed areas. Scale bars for all panels in [A] are 3 mm and 1.5 mm for all panels in [B].

Figure 4. Histomorphometric analyses of host tissue responses and wound healing outcomes. [**A**] Histomorphometric scoring matrix and [**B**] outcomes. Data in Panel B was acquired from N=4–7 animals per experimental group. Means ± standard deviation. For all markers, $p>0.05$ for post-repair buccal mucosa (BMG) vs post-repair bi-layer silk fibroin (BLSF) grafts as well as post-repair BLSF vs controls.

References

1. Verla W, Oosterlinck W, Spinoit AF, et al. A Comprehensive Review Emphasizing Anatomy, Etiology, Diagnosis, and Treatment of Male Urethral Stricture Disease. Biomed Res Int. 2019;18:9046430.

2. Cotter KJ, Hahn AE, Voelzke BB, et al. Trends in Urethral Stricture Disease Etiology and Urethroplasty Technique From a Multi-institutional Surgical Outcomes Research Group. Urology. 2019;130:167-174.

3. Payne SR, Anderson P, Spasojević N, et al. Male urethral stricture disease: why management guidelines are challenging in low-income countries. BJU Int. 2022;130:157-165.

4. Hoy NY, Chapman DW, Dean N, et al. Incidence and Predictors of Complications due to Urethral Stricture in Patients Awaiting Urethroplasty. J Urol. 2018;199:754-759.

5. Liao RS, Stern E, Wright JE, et al. Contemporary Management of Bulbar Urethral Strictures. Rev Urol. 2020;22:139-151.

6. Hughes M, Blakely S, Nikolavsky D. Advancements in transurethral management of urethral stricture disease. Curr Opin Urol. 2021;31:504-510.

7. Ali MM, Kamel M, Ragab A, et al. Holmium laser versus cold knife visual internal urethrotomy for management of short segment urethral stricture: a prospective randomized clinical trial. World J Urol. 2023;41:1897–1904.

8. Barbagli G, Fossati N, Montorsi F, et al. Focus on Internal Urethrotomy as Primary Treatment for Untreated Bulbar Urethral Strictures: Results from a Multivariable Analysis. Eur Urol Focus. 2020;6:164-169.

9. Yi YA, Rozanski AT, Shakir NA, et al. Balloon dilation performs poorly as a salvage management strategy for recurrent bulbar urethral strictures following failed urethroplasty. Transl Androl Urol. 2020;9:3-9.

10. Horiguchi A. Substitution urethroplasty using oral mucosa graft for male anterior urethral stricture disease: Current topics and reviews. Int J Urol. 2017;24:493-503.

11. Al-Qudah HS, Santucci RA. Extended complications of urethroplasty. Int Braz J Urol. 2005;31:315–323.

12. Wang A, Chua M, Talla V, et al. Lingual versus buccal mucosal graft for augmentation urethroplasty: a meta-analysis of surgical outcomes and patient-reported donor site morbidity. Int Urol Nephrol. 2021;53:907-918.

13. Qin D, Wang X, Mao Y, et al. Using of Single-Layer Porcine Small Intestinal Submucosa in Urethroplasty on a Beagle Model. Biomed Res Int. 2022;27:1755886.

14. Rashidbenam Z, Jasman MH, Hafez P, et al. Overview of Urethral Reconstruction by Tissue Engineering: Current Strategies, Clinical Status and Future Direction. Tissue Eng Regen Med. 2019;16:365-384.

15. Cao N, Song L, Liu W, et al. Prevascularized bladder acellular matrix hydrogel/silk fibroin composite scaffolds promote the regeneration of urethra in a rabbit model. Biomed Mater. 2018;14:015002.

16. Raya-Rivera A, Esquiliano DR, Yoo JJ, et al. Tissue-engineered autologous urethras for patients who need reconstruction: an observational study. Lancet. 2011;377:1175-1182.

17. Atala A, Danilevskiy M, Lyundup A, et al. The potential role of tissue-engineered urethral substitution: clinical and preclinical studies. J Tissue Eng Regen Med. 2017;11:3–19.

18. Palminteri E, Toso S, Preto M, et al. Small intestinal submucosa graft bulbar urethroplasty is a viable technique: results compared to buccal mucosa graft urethroplasty after propensity score matching. World J Urol. 2024;42:123.

19. Ortac M, Ekerhult TO, Zhao W, et al. Tissue Engineering Graft for Urethral Reconstruction: Is It Ready for Clinical Application? Urol Res Pract. 2023;49:11-18.

20. Aodi J, Ying L, Chengyang S, et al. Acellular dermal matrix in urethral reconstruction. Front Pediatr. 2024;12:1342906.

21. Lin D, Wang G, Song H, et al. Use of Acellular Dermal Matrix for Urethroplasty Coverage in Proximal Hypospadias Repair: a Pilot Study. Adv Ther. 2020;37:1425-1435.

22. Simsek A, Aldamanhori R, Chapple CR, MacNeil S. Overcoming scarring in the urethra: challenges for tissue engineering. Asian J Urol. 2018;5:69–77.

23. Sack BS, Mauney JR, Estrada CR Jr. Silk Fibroin Scaffolds for Urologic Tissue Engineering. Curr Urol Rep. 2016;17:16.

24. Chung YG, Tu D, Franck D, et al. Acellular bi-layer silk fibroin scaffolds support tissue regeneration in a rabbit model of onlay urethroplasty. PLoS One. 2014;9:e91592.

25. Algarrahi K, Affas S, Sack BS, et al. Repair of injured urethras with silk fibroin scaffolds in a rabbit model of onlay urethroplasty. J Surg Res. 2018;229:192-199.

26. Seth A, Chung YG, Gil ES, et al. The performance of silk scaffolds in a rat model of augmentation cystoplasty. Biomaterials. 2013;34:4758-4765.

27. NRC (National Research Council). Guide for the Care and Use of Laboratory Animals. Washington (DC): The National Academies Press;2011.

28. United States Code [Internet]. Animal Welfare Act. Title 7 - Agriculture. Chapter 54 - Transportation, Sale, and Handling of Certain Animals; Sections 2131–2159. Available from: https://uscode.house.gov/view.xhtml?path=/prelim@title7/chapter54&edition=prelim.

29. Code of Federal Regulations [Internet]. Animal Welfare Regulations. Title 9 – Animals and Animal Products. Chapter 1 - Animal and Plant Health Inspection Service, Department of Agriculture. Subchapter A - Animal Welfare; Parts 1-3. Available from: https://www.ecfr.gov/current/title-9/chapter-I/subchapter-A.

30. American Veterinary Medical Association [Internet]. AVMA Guidelines for the Euthanasia of Animals. Available from: https://www.avma.org/resources-tools/avma-policies/avma-guidelines-euthanasia-animals.

31. Oliva P, Delcelo R, Bacelar H, et al. The buccal mucosa fenestrated graft for Bracka first stage urethroplasty: experimental study in rabbits. Int Braz J Urol. 2012;38:825-32.

32. Andersen HL, Duch BU, Nielsen JB, et al. An experimental model for stricture studies in the anterior urethra of the male rabbit. Urol Res. 2003;31:363–367.

33. Faydaci G, Tarhan F, Tuncer M, et al. Comparison of two experimental models for urethral stricture in the anterior urethra of the male rabbit. Urology. 2012;80:e7-11.

34. Meria P, Anidjar M, Brouland JP, et al. An experimental model of bulbar urethral stricture in rabbits using endoscopic radiofrequency coagulation. Urology. 1999;53:1054–1057.

35. Chen Q, Cheng W, Cao J, et al. An experimental model for stricture studies in the anterior urethra of the male canine. J Mod Urol. 2008;13:303–305.

36. Adamowicz J, Van Breda SV, Kloskowski T, et al. Constructing artificial urinary conduits: current capabilities and future potential. Expert Rev Med Devices. 2019;16:135-144.

37. Kim UJ, Park J, Kim HJ, et al. Three-dimensional aqueous-derived biomaterial scaffolds from silk fibroin. Biomaterials. 2005;26:2775-85.

38. Wang Y, Rudym DD, Walsh A, et al. In vivo degradation of three-dimensional silk fibroin scaffolds. Biomaterials. 2008;29:3415-28.

39. Tu DD, Chung YG, Gil ES, et al. Bladder tissue regeneration using acellular bi-layer silk scaffolds in a large animal model of augmentation cystoplasty. Biomaterials. 2013;34:8681-8689.

40. Brown BN, Badylak SF. Extracellular matrix as an inductive scaffold for functional tissue reconstruction. Transl Res. 2014;163:268-285.

41. Mauney JR, Cannon GM, Lovett ML, et al. Evaluation of gel spun silk-based biomaterials in a murine model of bladder augmentation. Biomaterials. 2011;32:808–18.

42. Altman GH, Diaz F, Jakuba C, et al. Silk-based biomaterials. Biomaterials. 2003;24:401-16.

43. Ceonzo K, Gaynor A, Shaffer L, et al. Polyglycolic acid-induced inflammation: role of hydrolysis and resulting complement activation. Tissue Eng. 2006;12:301-8.

44. Splieth CH, Sumnig W, Bessel F, et al. Prevalence of oral mucosal lesions in a representative population. Quintessence Int. 2007;38:23–9.

45. Kinnaird AS, Levine MA, Ambati D, et al. Stricture length and etiology as preoperative independent predictors of recurrence after urethroplasty: a multivariate analysis of 604 urethroplasties. Can Urol Assoc J. 2014;8:E296–E300.

46. Gundogdu G, Nguyen T, Eijansantos M, et al. Development of male and female models of long urethral strictures in swine. Surg Open Sci. 2023;16:205-214.

47. Andrich DE, Mundy AR. Substitution urethroplasty with buccal mucosal-free grafts. J Urol. 2001;165:1131–1133.

48. Barbagli G, De Angelis M, Palminteri E, et al. Failed hypospadias repair presenting in adults. Eur Urol. 2006;49:887–894.

Reference Annotations

*1. Verla W, Oosterlinck W, Spinoit AF, et al. A Comprehensive Review Emphasizing Anatomy, Etiology, Diagnosis, and Treatment of Male Urethral Stricture Disease. Biomed Res Int. 2019;18:9046430.

This article provides a contemporary survey of approaches and limitations in the management of urethral stricture disease.

*14. Rashidbenam Z, Jasman MH, Hafez P, et al. Overview of Urethral Reconstruction by Tissue Engineering: Current Strategies, Clinical Status and Future Direction. Tissue Eng Regen Med. 2019;16:365-384.

This article describes current advantages and disadvantages of various tissue engineering approaches for urethral reconstruction.

**16. Raya-Rivera A, Esquiliano DR, Yoo JJ, et al. Tissue-engineered autologous urethras for patients who need reconstruction: an observational study. Lancet. 2011;377:1175-1182.

This article describes the performance of a first in man, clinical trial of a cell-seeded, tubular implant for urethral reconstruction.

** 24. Chung YG, Tu D, Franck D, et al. Acellular bi-layer silk fibroin scaffolds support tissue regeneration in a rabbit model of onlay urethroplasty. PLoS One. 2014;9:e91592.

The results of this study demonstrate that bi-layer silk fibroin scaffolds promote similar degrees of urethral tissue regeneration in comparison to conventional small intestinal submucosal scaffolds, but with reduced immunogenicity.

**25. Algarrahi K, Affas S, Sack BS, et al. Repair of injured urethras with silk fibroin scaffolds in a rabbit model of onlay urethroplasty. J Surg Res. 2018;229:192-199.

The results in this article demonstrate the ability of bi-layer silk fibroin grafts to support the repair of previously damaged urethral tissues.

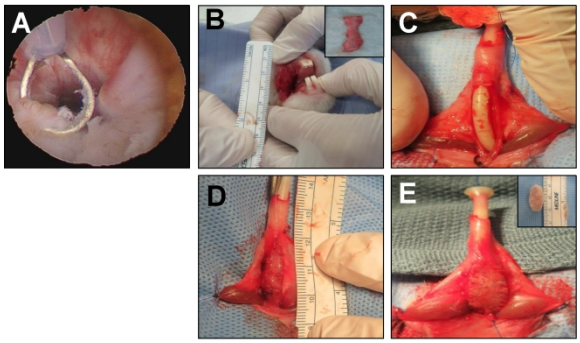

Figure 1

Figure 1. Rabbit model of urethral stricture disease and urethroplasty. [A] Urethroscopic view of urethral mucosa during electrocoagulation injury. [B] Autologous buccal mucosa harvest with inset showing implant dimensions. [C] Creation of urethral defect. [D, E] Ventral onlay urethroplasty with buccal mucosal graft [D] and bilayer silk fibroin (BLSF) scaffold [E] following stricture formation. Inset in [E]: BLSF matrix prior to implantation.

338x190mm (300 x 300 DPI)

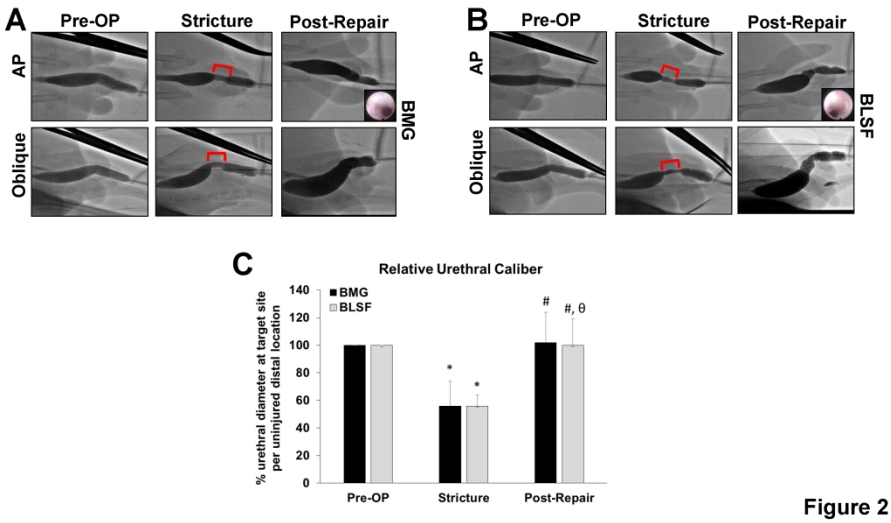

Figure 2

Figure 2. Imaging evaluations of urethral injury and repair responses. [A, B] Longitudinal retrograde urethrographic (RUG) analysis [Anterior/Posterior (AP) and oblique views] of representative animals at pre-operative baseline, after electrocoagulation injury demonstrating stricture formation (brackets), and at 3 months post-repair with buccal mucosal (BMG) [A] or bi-layer silk fibroin (BLSF) [B] grafts. Insets: urethroscopic images of repaired urethras at harvest. [C] Quantitation of relative urethral calibers calculated from RUG evaluations. Means ± standard deviation. (*) = $p<0.05$ compared to respective pre-operative baseline. (#) = $p>0.05$ compared to respective pre-operative baseline. (θ), $p=0.83$ in comparison to rabbits reconstructed with BMG grafts. Data in Panel C was acquired from N=4–7 animals per experimental group.

338x190mm (300 x 300 DPI)

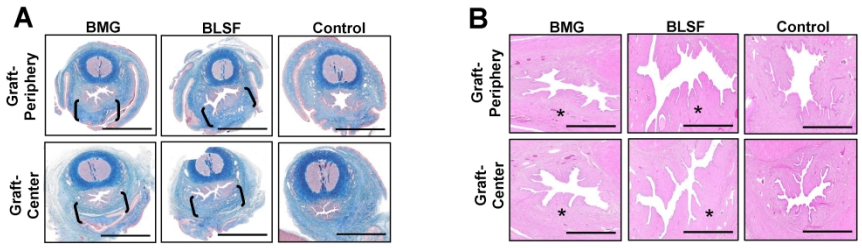

Figure 3

Figure 3. Histological evaluations of urethral neotissues and controls. [A, B] Photomicrographs of representative urethral cross-sections from rabbits repaired with buccal mucosal (BMG) or bi-layer silk fibroin (BLSF) grafts at 3 months post-op as well as controls stained with Masson's trichrome [A] and hematoxylin and eosin [B]. Axial periphery and central views of neotissues and controls are displayed in all panels. Brackets and asterisks denote reconstructed areas. Scale bars for all panels in [A] are 3 mm and 1.5 mm for all panels in [B].

338x190mm (300 x 300 DPI)

A

Histomorphometric Scoring Matrix	
Score	Overall Inflammation and Inflammatory Cell Types
0	Absent
1	Minimal; Scattered inflammatory cells (~2-3 layers or less)
2	Mild; Light infiltrates a few cells thick (~2-3 layers or more)
3	Moderate; Widespread infiltrates of larger aggregates
4	Overwhelming infiltrates with effacement of tissue architecture
Score	Epithelial Erosion/Loss
0	0%; Confluent luminal epithelialization
1	Minimal denudation with 75% luminal epithelialization
2	Mild to moderate denudation with 50-75% luminal epithelialization
3	Moderate denudation with 25-50% luminal epithelialization
4	Marked denudation with <25% epithelial coverage
Score	Submucosal Hemorrhage, Necosis, and Fibrosis
0	No response
1	Minimal/focal/barely detectable
2	Mild/focal or rare multifocal/slightly detectable
3	Moderate/multifocal to confluent/easily detectable
4	Marked/diffuse/overwhelming presence

B

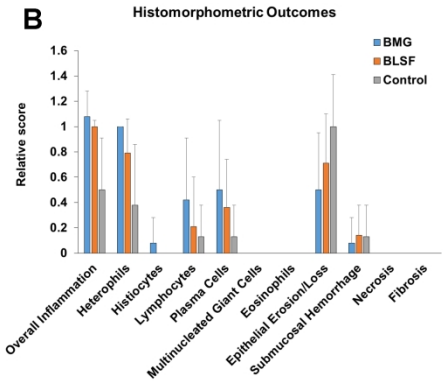

Figure 4

Figure 4. Histomorphometric analyses of host tissue responses and wound healing outcomes. [A] Histomorphometric scoring matrix and [B] outcomes. Data in Panel B was acquired from N=4–7 animals per experimental group. Means ± standard deviation. For all markers, $p>0.05$ for post-repair buccal mucosa (BMG) vs post-repair bi-layer silk fibroin (BLSF) grafts as well as post-repair BLSF vs controls.

338x190mm (300 x 300 DPI)